EUROVENT 8/10 - 1992

PRACTICAL GUIDELINES
for
FLOW-GENERATED NOISE IN SELECTED ELEMENTS

EUROVENT 8/10

First edition 1992

This document has been prepared by EUROVENT WG 8 « ACOUSTICS »

Published by EUROVENT/CECOMAF
15 rue Montorgueil
F-75001 PARIS
Tel 33 1 40 26 00 85
Fax 33 1 40 26 01 26

FORWARD

This document has been elaborated by EUROVENT simply to provide guidelines concerning the material discussed herein. The subject of this brochure is "Flow-generated noise," and it is not our intention here to present the reader with solutions to all flow noise problems.

Nonetheless, it will make the user aware of many of the problems and will indicate an order of magnitude for the noise levels in question. Some of the data presented are in-depth, while others are more general and have been taken from manufacturers' catalogues. We hope this is a valuable, concise document which provides indices for a multitude of situations.

The graphs contained in this brochure were taken from original papers, and the decision was made to reproduce them as initially published. Although it might have been possible to present them in a more unified and professional manner, we felt it preferable to leave them with the original "authors' touch."

Throughout this document, spread data between results and indicated trends is presented, permitting the reader to understand that there exist inherent uncertainties in the field and that "not all of the answers have been found."

AVANT-PROPOS

Ce document, établi par EUROVENT, a pour but de présénter des résultats relatifs au bruit généré par l'écoulement à travers un certain nombre de composants aérauliques. Il ne permettra pas au lecteur de traiter tous les problèmes de bruit d'écoulement auxquels il est susceptible d'être confronté.

Il fournit cependant des données chiffrées, tirées de la littérature existante ou de catalogues constructeurs, qui permettent d'appréhender les phénomènes en jeu et de donner des ordres de grandeur utiles pour un grand nombre d'applications pratiques.

Les figures présentées dans cette note sont directement reproduites à partir des textes originaux afin de laisser aux auteurs concernés la part de responsabilité qui leur incombe dans la publication des résultats.

Tout au long de la présentation, on a également fait figurer la dispersion des résultats relevées. Ceci permet au lecteur d'apprécier les incertitudes inhérentes aux données présentées et de lui faire comprendre que "tout n'est pas encore totalement résolu."

VORWORT

Dieses Dokumet wurde von Eurovent erarbeitet, um Richtlinien, und nicht mehr als das, für die dargestellten Komponenten an die Hand zu geben. Das Thema sind strömungserregte Geräusche, wobei nicht daran gedacht ist, auf den folgenden Seiten eine Beschreibung zu liefern, die dem Leser die Möglichkeit gibt, alle Probleme von Strömungsgeräuschen zu lösen.

Es werden dennoch hiermit viele Probleme bewuBt gemacht und hilfreiche Hinweise für die Beurteilung der betreffenden GeräuschgröBen gegeben. Die Qualität der Daten ist sehr unterschiedlich, da manche sehr genau, einige dagegen weniger genau sind und einige aus Herstellerkatalogen entnommen wurden. Trotzdem ist es ein wertvolles und umfassendes Dokument, welches für viele gegebene Fälle die GröBenordnung der Probleme deutlich macht.

Die in diesem Dokument enthaltenen graphischen Darstellungen wurden Originalunterlagen entnommen, wobei entschieden wurde, sie wie bereits veröffentlicht abzudrucken. Es ist klar, daß Eurovent aus der Menge dieser Reproduktionen eine eigene mehr professionell erscheinende Uterlage hätte erarbeiten können. Dabei wäre aber eventuell die "Handschrift" der eigentlichen Autoren verloren gegangen.

In dieser Unterlage bleibt bei der Vielzahl der Daten der Zusammenhang zwischen festgestellten Ergenbnissen und dargestellten Trends erhalten. Dadurch werden dem Leser die gegebenen Toleranzräume bewußt gemacht und ihm vermittelt, daß "nicht alle Probleme bis zum letzten erforscht sind."

SUMMARY

0 - INTRODUCTION

Aerodynamic noise is generated in boundary layers, discontinuities and deflections of flow, e.g. in jets, wakes, elbows, absorption silencers, resonator silencers, branch take-offs, air modulation units and other duct elements.

The peak frequencies of the aerodynamically generated noise depend on the geometry of the devices, the turbulence level and the velocity of the flow. These parameters can usually be combined into the dimensionless Strouhal number

$$S = fd/u$$

in which d is a characteristic length, f is the peak frequency and u is the velocity of the flow.

The intensity of flow-generated noise is proportional to between the fifth and sixth power of the local flow velocity in the duct.

Aerodynamic noise can be kept low if the flow velocity is low and if abrupt changes in area or direction of flow are avoided.

Special problems are stressed in this document, and in particular, the influence of flow on propagation of noise in ducts, on the effectiveness of absorption silencers and Helmholtz resonators, on the vortex shedding of plates and on the branching of side ducts from the main duct.

1 - NOISE SOURCES IN DUCTED SYSTEMS

The table below lists some of the noise sources found in ducted systems, as shown in Figure 1.

1	-	Free turbulent flow from the damper blade
2	-	Friction of the flow on the damper casing *(boundary noise)*
3	-	Turbulent boundary layer flow on the duct wall
4	-	Turbulence at elbows
5	-	Turbulence at junctions
6	-	External fluctuating excitation forces
7	-	Turbulence behind nozzles, orifice plates and constrictions
8	-	Bellows

9 - Acoustical resonance in the working fluid

10 - Turbulence behind expansion or contractions

11 - Structure borne noise and vibration from the connected system.

2 - NOISE GENERATION FROM DAMPERS

2.1 Fluctuating pressure *(Figure 2)*

Gate valve :

Curve 1 for large openings shows the behaviour of turbulent flow qualitatively obeying the resistance law concerning ducts.

Curve 2 for small openings shows the behaviour of the transition laminar toward flow duct turbulences thus, indicating the influence of the friction effect of the duct wall.

2.2 Frequency spectrum *(Figure 3)*

Gate valve :

The fluctuating pressure is correlated with

$S_{hmax}\, M^{*2}/\sqrt{Re}$ where the Strouhal number is :

$$S_{hmax} = \frac{f.hmax}{U}$$

with U = average velocity in the opening

and Mach number

$$M^* = \frac{U}{a^*}$$

with

a^* = critical velocity of sound

The Reynolds number Re indicates the friction effect on the duct wall.

2.3 Noise propagation in the downstream duct *(Figure 4)*

The noise generated by the wall flow of the gate valve propagates into the downstream duct with a strong unsteadiness behind the valve. Therefore, the main attenuation of the noise takes place only within a one-diameter distance from the valve *(see Figure 4)*.

The low frequency components which usually accompany the turbulent activity of a free jet are therefore strongly reduced.

The table in Figure 4 reveals that the attenuation of noise per 1 m duct length is dependent on the duct diameter. The larger the diameter, the higher the attenuation. This is because of the radiation of the duct wall surface into the surroundings. The larger the surface, the stronger the radiation loss.

3 - NOISE GENERATION IN T-JUNCTIONS

Two extreme cases are considered.

Figure 5a

In case 1, is all flow is led into the deflected branch II, while in case 2, there is only flow into duct III without deflection. The average noise reduction in branch II and that in duct III are nearly equal for each of the two cases, namely :

> 1.5 - 4 dB for case 1 *(just below the theoretical value of 3 dB)*, 2 - 7 dB for case 2 *(exceeding the theoretical value of 3 dB)*.

In case 1, additional noise is generated by turbulence of the deflected flow, while in case 2, noise is reduced by mismatching.

Figure 5b

This shows sound power levels of branch take-offs from a 900 x 300 mm duct through a plain tee. Volume flow rates for the main duct vary from 2.5 to 9 m^3 / s.

Figure 5c

Here we see the influence of a coned connection in reducing the noise from abrupt connections.

Figure 5d

This reveals the effect of rounding of the corners upon noise reduction, with $r/D_B = 0.15$ as a reference.

Figure 5e

This figure shows noise spectrum changes with the ratio of the velocities in the main duct and branch duct as parameter, at a rounding of corners of

$r/D_B = 0.15$.

Figure 5f

This figure summarizes further guidelines for minimizing flow-generated noise at T junctions.

4 - EFFECT OF FLOW DIRECTION UPON NOISE INTENSITY

For the propagation of sound with flow through a duct with acoustically hard walls, the amplitude in the upstream direction, P-, is higher than in the downstream direction, P+ *(see Figure 6 for 1000 and 1477 Hz)*. The difference increases monotonically with the Mach number. For frequencies above 1000 Hz, this trend holds true.

The attenuation of a rectangular absorption silencer at 40 m/s passage velocity is higher for the reverse flow in the low frequency range below 1000 Hz, but lower for the reverse flow in the high frequency range above 1000 Hz *(Figure 7)*. The reason for this is that the short-wavelength noise *(high frequencies)* is refracted by the reverse flow away from the absorption material of the wall, but is refracted by the forward flow into the absoption material *(Figure 7)*. The changeover of flow direction effects occurs at a frequency which is just about the cut-off frequency which for this passage size.

A similar example, for cylindrical silencers is given in Figure 8. The higher attenuation at low frequencies that accompanies the larger diameter is consistent with the general property of dissipative parallel baffle silencers, which have a maximum attenuation for diameters on the order of a wave length.

Further experimental results are shown in Figures 9, 10 and 11. The attenuation decrease with the forward flow is greater the narrower the duct section. See Figure 12 for frequency ranges 125 to 2000 Hz.

5 - FLOW-GENERATED NOISE IN DUCTS

The dimensionless sound power spectrum P (w) of the duct-wall pressure fluctuations due to turbulent boundary layer decreases with the Strouhal number wd^*/u, or fd^*/u, where d^* = displacement thickness of the boundary layer, u = free stream velocity, tw = mean wall stress *(Figure 13a and 13b)*.

The noise radiated by a turbulent boundary layer is given in Figure 14. The sound power spectra of 600 mm x 600 mm straight steel duct for air flow velocities of 10, 15 and 25 m/s are given in Figure 15. Measures to reduce the probability of drumming in large aspect ratio rectangular ducts are given in Figure 16, either by means of partitions or perforated plates in order to smooth or break up the large-sized turbulence of the flow.

6 - FLOW-GENERATED NOISE IN SILENCERS

Some data concerning flow-generated noise in silencers are summarized in this section.

Figure 17 shows the flow-generated noise in a rectangular duct silencer for forward and reverse flow. The reverse flow noise is smaller in the low frequency range, but larger in the high frequency range. This trend is similar to the results given in the previous section on the effect of flow on attenuation.

Figure 18 shows the effect of the aerodynamic shape of the entry nose of a silencer splitter. The flat nosed splitters create much more noise than the round nosed splitters, especially in the lower frequency range below 2000 Hz.

7 - FLOW-INDUCED NOISE IN ELBOWS

A single splitter turning vane can reduce the noise in the low and high frequency ranges, *(Figure 19)*.

Short chord turning vanes are capable of reducing the noise in the low and the high frequency range, *(Figure 20)*. But if the trailing edge of the vane is inadequately formed, the noise in the middle frequency range can be increased *(Figure 20)* due to the formation of a Karman vortex street in the wake. Karman vortices can excite the vane to vibrate in resonance.

Figure 21 shows the approximate level of sound power generated by air flowing through elbows with vanes at 10 m/s.

Figure 22a gives the pressure drop coefficients of elbows of different forms. The flow-induced noise can be considered proportional to the pressure drop coefficient.

Figure 22b gives additional guidance for minimizing flow-generated noise in elbows and bends.

8 - FLOW-INDUCED VIBRATIONS ON PLATES OR GUIDE VANES

If a flow streams along a plate or a guide vane, a wake with Karman vortex street can be generated. The fluctuating dynamic force of this Karman vortex can excite the plate or the guide vane to vibrate in resonance.

The excitation can be kept to a minimum if the shape of the trailing edge of the plate or the vane is adequately constructed, *(Figure 23)*.

The diagram shows the excitation in relative displacement against the ratio **s/h**, where **s** is the length of the trailing edge and **h** is the thickness of the plate or vane.

Concerning the frequency of excitation :

- For short plates, plate thickness, h will enter into the Strouhal equation.

• For long plates, the additional thickness of the exit boundary layer will enter into the Strouhal equation.

9 - FLOW-GENERATED NOISE AT DISCONTINUITIES OF DUCT

The flow at a sudden expansion of duct produces turbulence and vortices, which cause pressure fluctuation and noise radiation. Figure 24 shows the spectra of such a pressure fluctuation with the Strouhal number as the abscissa :

$$S = \frac{f \cdot (D - d)}{u}$$

and the distance from the discontinuity as a dimensionless parameter :

L/(D-d)

The maximal pressure fluctuation occurs when this parameter is approximately equal to 4, corresponding to flow reattachment.

Figure 27 displays the noise generation of the discontinuity as a function of flow velocity for two kinds of sudden section reduction :

600 x 600 to 600 x 200 mm
600 x 600 to 200 x 200 mm

Reduction on two sides makes considerably more noise than reduction on one side.

The improvement achieved with a gradual reduction is much more marked for the two sided discontinuity change, an improvement of about 30 dB over the entire frequency range is achieved for the reduction of

600 x 600 to 200 x 200 mm

If the sudden change in the cross section is made by expansion on one side but by reduction on the other, then a gradual change can improve the situation, especially in the high-frequency range above 500 Hz. *Figure 26* indicates this for the section change :

from 600 x 600 to 300 x 900 mm

Another example for an extremely sudden section change

from 600 x 600 to 200 x 1200 mm

is given in *Figure 29*. the improvement by the gradual section change can reach 30 dB, again over the whole frequency range again.

Figure 28 summarizes further guidelines for minimizing flow-generated noise at cross-section changes.

10 - FLOW-GENERATED NOISE FROM BUTTERFLY DAMPER

If the butterfly damper blade is completely opened so that the incidence angle of the flow to the blade is zero, the noise is generated by the boundary layers and the wake, which is generally composed of a Karman vortex street.

The noise spectrum given in *Figure 29* shows a pronounced peak at 500 Hz for high flow velocities. If the entire thickness of the butterfly blade, including the boundary layers on its two sides, is assumed to be 20 mm, then the Strouhal number for the velocity of 30 m/s :

$$S = \frac{fd}{u} = \frac{500 \times 0.02}{30} = 0.3$$

corresponds well to the excitation of a Karman vortex street. In addition, the frequency of 500 Hz with a wavelength of :

$$l = \frac{330}{500} = 0.66 \text{ m}$$

corresponds to an acoustical resonance for the lateral gas column in the duct *(600 x 600 mm)*. Therefore, the peak is especially strong.

When the butterfly blade is slightly closed to an incidence angle of = 15 ° to the flow, the spectrum is generally raised by about 10 dB, see (*Figure 30.*).

When the butterfly blade is further closed to an incidence angle of 45 ° - (Figure 31) the flow is completely separated behind the blade. Now, the gap of 90 mm between the blade and the wall will be an important parameter in addition to the projected width of the blade. The vortices in the dead zone immediatly behind the blade cause a noise increase in the very low frequency range below 125 Hz. Because of the contraction, the effective gap can be reduced to about 50 mm and the effective velocity of the flow can be raised by a factor of :

$$\frac{300}{50} = 6$$

Now, the maximum velocity of 15 m/s in Figure 31 is raised to about 100 m/s. The Strouhal number gap for the peak frequency of 500 Hz would be :

$$S_{gap} = \frac{500 \times 0.05}{\quad} = 0.25$$

This value agrees well with the theory

An example of sound generated by the Karman vortex street of four 13 mm diameter rods in a flow of 25 m/s is given in Figure 32. The frequency peak in the 500 Hz octave band corresponding to a transverse resonance of the duct *(600 x 600 mm)* has a Strouhal number of -

$$S_{gap} = \frac{500 \times 0.013}{25} = 0.26$$

This Strouhal number agrees well for the excitation of a Karman vortex street. Therefore, the peak reaches 20 dB above the neighboring frequency range.

11 - STREAMLINE-SPLITTER SILENCER WITH SMALLEST FLOW-GENERATED NOISE

A streamline-splitter silencer abrupt section change has the smallest flow-generated noise. The attenuation achieved by means of such a silencer can therefore be very high, *(Figure 33)*.

12 - INFLUENCE OF FLOW ON THE DAMPING EFFECT OF A SIDE-BRANCH - HELMOLTZ RESONATOR

A normal side-branch Helmholtz resonator is only effective for the acoustical case without flow. If there is a flow in the main duct, the damping effect will be reduced. The reason for this is that the vibrating gas column through the neck of the resonator is disturbed by the turbulence created by the cross flow of the main duct. This turbulence can be weakened by lining the duct near the necks, *(Figure 34)*. The damping can be kept high at a resonance frequency up to a flow velocity of 20 to 80 m/s.

It is to be noted that the resonance frequency of the Helmholtz resonator is raised by the flow (see diagram *(E)* , *Figure 34*).

13 - JET NOISE

The noise radiated by the following jets are given in *Figure 35* with the Lighthill parameter as the abscissa. Clearly three regions exist :

1. Turbo jet *(no reheat)* and air jet model.

2. Rocket and turbo jet *(with reheat)*.

3. Air multi-jets with low velocities
(air conditioning zone).

14 - NOISE RADIATION OF A PLATE EXCITED BY A TURBULENT BOUNDARY LAYER

The acoustical power radiated by a plate due to excitation of the turbulent boundary layer *(plate thickness : 0.0015 m, 0.003 m and 0.006 with flow velocities of 30 and 55 m/s)* is shown in *Figure 36*.

15 - REFERENCES

1 - ASHRAE HANDBOOK, 1987, Chapter 52, "Sound and Vibration Control."

2- BAUER, A.B., and CHAPKIS, R.L., 1977, Noise Generated by boundary-layer interaction with perforated acoustic liners, J. Aircraft, Vol. 14, pp.157-160.

3 - BIOLLEY, A., Hilfsmittel zur Verringerung der Verluste in scharfen Krümmern. Schweizerische Bauzeitung, 1941, pp.85.

4 - BROCKMEYER, H., Akustik für den Lüftungs-und Klimaingenieur, Berichte aus der Kälte-, Wärme;, Klima-und Regeltechnik, Verlag C.F. Müller, 1971, pp.62-74.

5 - CHEN, Y.N., and FLORJANCIC, D., Karman-vortex-induced vibrations on guide vanes with slender trailing edges. The Institution of Mechanical Engineers, Conference on Vibration and Noise in Pump, Fan and Compressor Installations, September 16-18, 1975, University of Southampton.

6 - CHEN, Y.N., Baylac, G., and Walther, R., Guide vane vibrations caused by wakes and blower noise. Part 1: The vortex degeneration in the asymmetrical wakes. To be presented at the ASME-Vibration Conference, 1975.

7 - CHEN, Y.N., Noise generated by multi-jets of acoustic tiles, Congress of the International Institute of Refrigeration, Vienna, 1973, Paper E1.

8 - CHEN, Y.N., Lateral Helmholz resonator silencer with turbulence absorption. The Institution of Mechanical Engineers, Proceedings, 1967-68, Vol. 182, Part 1, second paper.

9 - DAVIES, H.G., Sound from turbulent-boundary-layer-excited panels. Journal of Acoustical Society of America, Vol. 49, 1971, N° 3, (Part 2), pp. 878-889.

10 - DITTMAR, R., 1987, Schallentschung und-ausbreitung in Robrleitingen, Marchinenbautechnik,Vol., pp. 210-215.

11 - ECK, B., Technische Strömungslehre, Springer Verlag, 1961, p. 231.

12 - FLEISCHER, F.1985, Gesichtspunke bei der Dimensionierung und Auswahl von Abgarschalldampfern, MTZ, Vol. 46.

13 - FRY, A., et al., Noise Control in Building Services, Pergamon Press 1988.

14 - GERBER, O. Die Geräuschbildung in Lüftern und ihre Dämpfung Lärmbekämpfung, vol. 1, 1957, pp. 93-101.

15 - GIBERT, R.J., Sources de fluctuations de pression au niveau de singularites et propagation dans les écoulements en charge, Proceedings CEA-EDF, N° 17, Symposium on Aéro-hydro-elasticité, 4-8.
Septembre 1972, at Ermenonville, France, pp. E 14-1 to E 14-35, Eyrolles 1973.

16 - HAY, J.A., Problems of cabin noise estimation for supersonic transports. Journal of Sound and Vibration, vol. 1 1964.

17 - HIRSCHORN, M., 1974, The Aeroacoustic rating of silencers for "forward" and "reverse" flow of air and sound," Noise Control Engineering, Winter 1974, pp. 25-29.

18 - HIRSCHORN, M., 1988, Compendum of Noise Control Engineering, Part II, Sound and Vibration, February 1988, pp. 16-28.

19 - INGARD, U., and Singhal, V.K., Upstream and downstream sound radiation into a moving fluid. Journal of Acoustical Society of America, vol. 54, 1973, N° 5, pp. 1343-1346.

20 - JUNGOWSKI, W.M. and SELEROWICZ, W.C., 1981, Theory and operation of a low noise throttering - Venting device noise control engineering, September-October 1981, pp. 86-94.

21 - KO, S.H., Sound attenuation in acoustically lined circular ducts in the presence of uniform flow and shear flow. Journal of Sound and Vibration, vol. 22, 1972, N° 2, pp. 193-210.

22 - KO, S.H., Sound attenuation in lined rectangular ducts with flow and its application to the reduction of aircraft engine noise. Journal of Acoustical Society of America, Vol. 1971, pp. 1418.

23 - MAESTRELLO, L. Measurements and analysis of the response field of turbulent boundary layer excited panels. Journal of Sound and Vibration, vol. 2, 1965, N° 3, pp. 270-292.

24 - MAESTRELLO, L. Use of turbulent model to calculate the vibration and radiation responses of a panel, with practical suggestions for reducing sound level. Journal of Sound and Vibration, vol. 5, 1967, N° 3, pp. 407-448.

25 - MECHEL, Fr., Schalldämpfung und Schallverstärkung in Luftströmungen durch absorbierend ausgekleidete Kanäle. Acustica, vol. 10, 1960, N° 3, pp. 133-148.

26 - MURMAM, H., 1976, Schalldämpfung und Schalldämmung un Lüftungstechnschen Anlagen. Waser, Luft und Betrieb. vol. 20, pp. 543-548.

27 - RIBNER, H.S., Quadrupole correlations governing the pattern of jet noise. University of Toronto, Institute for Aerospace Studies. UTIAS Report N° 128, AFOSR 67-2159, 1967.

28 - RIBNER, H.S., 1981, Perspectives on jet noise, AIAA Journal, vol. 19, pp. 1513-1526.

29 - SCHMIDT, L. 1976, Der Einfllufs eimes 90° - Robrerummer auf die Schallemission emes Axialventilators, Luft und Kältstechnik pp. 287-290.

30 - Silencers 1982. Journal of Sound and Vibration, August 1982, pp. 14-17.

31 - TACK, D.H. and LAMBERT, R.F., Influence of shear flow on sound attenuation in a lined duct. Journal of Acoustical Society of America, vol. 38-1965, N° 4, pp. 655-666.

32 - TAM, CHR, K.W., Intensity spectrum and directivity of turbulent boundary layer noise. Journal of Acoustical Society of America, vol. 57, 1975, N° 1 pp. 25-33.

33 - VDI 3733 Gerausche bei Rohrlistungen.

Figure 1

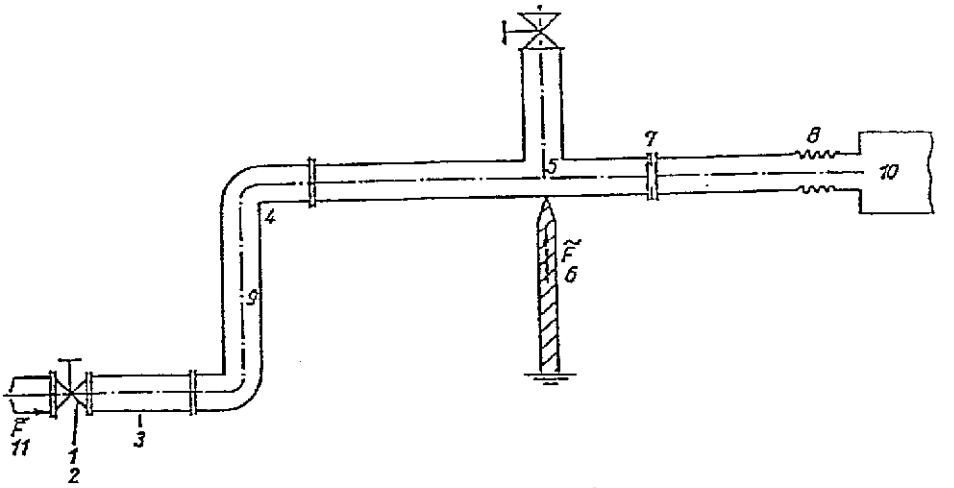

Figure 2

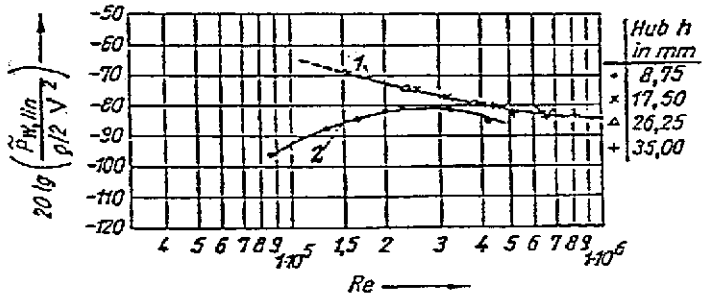

$$\frac{\tilde{p}_{w,lin}}{\frac{\rho}{2}\bar{V}^2} \sim \frac{dp_{St}/d(l/D)}{\frac{\rho}{2}\bar{V}^2}$$

$\tilde{p}_{w,\,lin}$ Acoustic pressure at the wall

$\bar{V}$ mean velocity

ρ density

$Re = \frac{hV}{\eta}\rho$

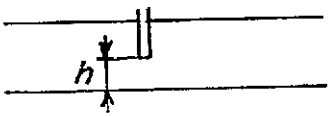

curve 1 for large gap : turbulent

curve 2 for small gap : transition laminar-turbulent

Figure 3

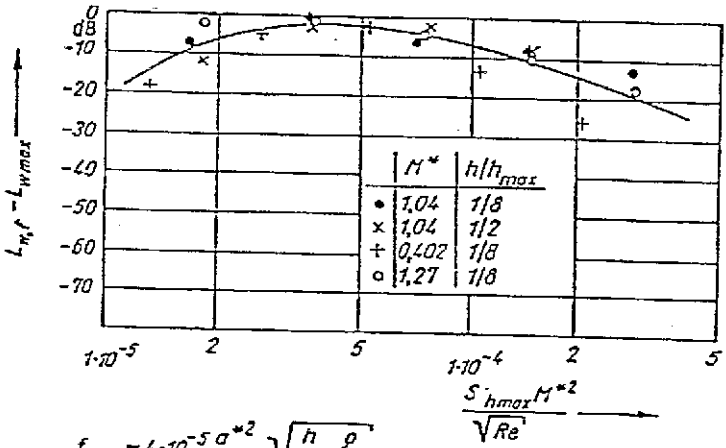

$$f_{max} = 4 \cdot 10^{-5} \frac{a^{*2}}{h_{max}} \sqrt{\frac{h}{v} \frac{\rho}{\eta}}$$

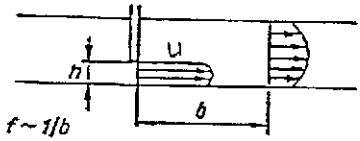

$f \sim 1/b$

$b \sim \left(\frac{u}{n}\right)^{\alpha}$; Measure: $\alpha = \frac{1}{2}$

Figure 4

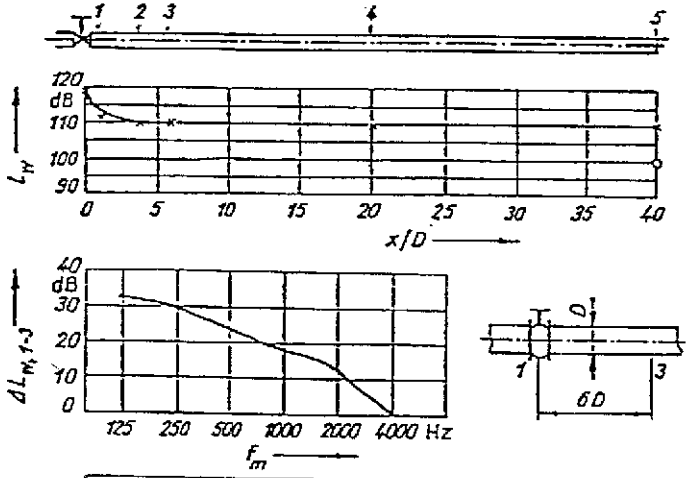

D in mm	ΔL/1m dB/m
52	0,20
80	0,31
100	0,35
150	0,55
400	1,0

Figure 5a

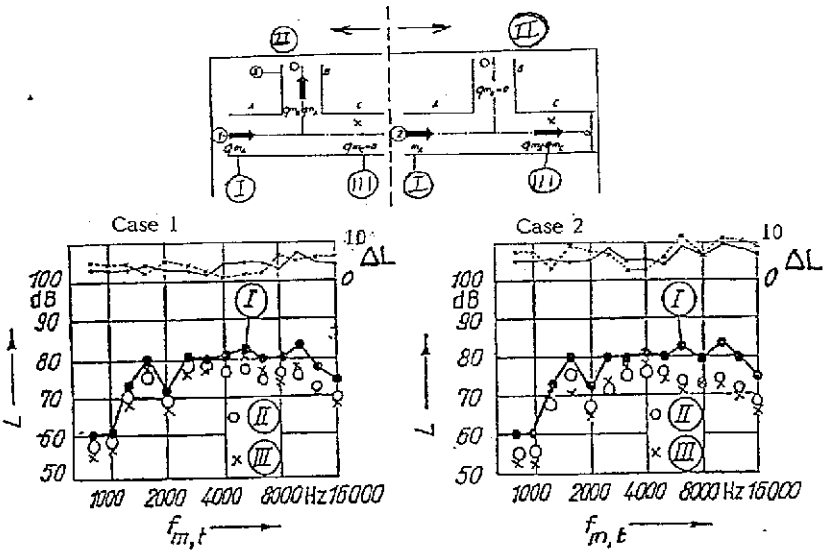

D = 100 mm; qm_A = 0,9 kg/s

Natural cross mode frequency : 1700 Hz

Figure 5 b

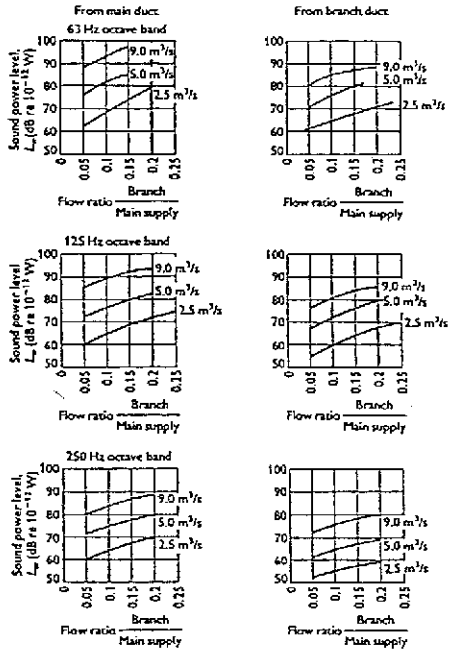

Figure 5c

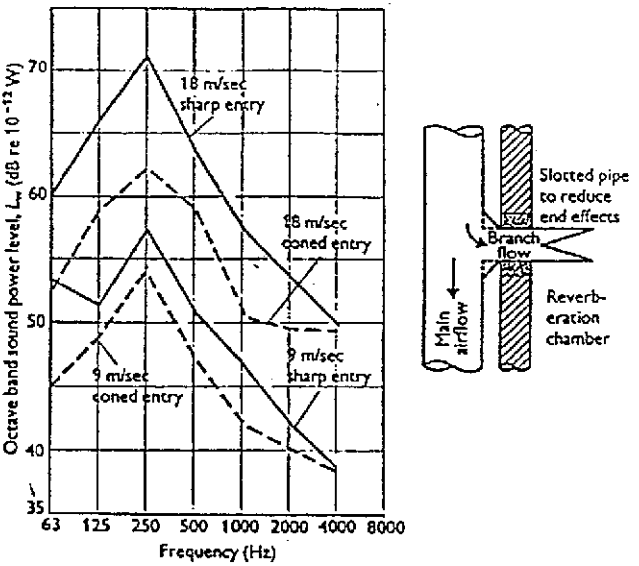

Figure 5d

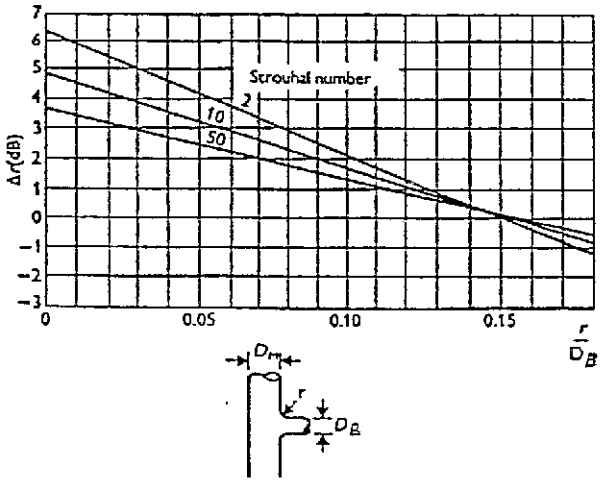

Figure 5e

The characteristic spectra K, are plotted in as a function of the Strouhal number with the velocity ratio U_M ·

U_B

as parameter for r = 0.15

D_B

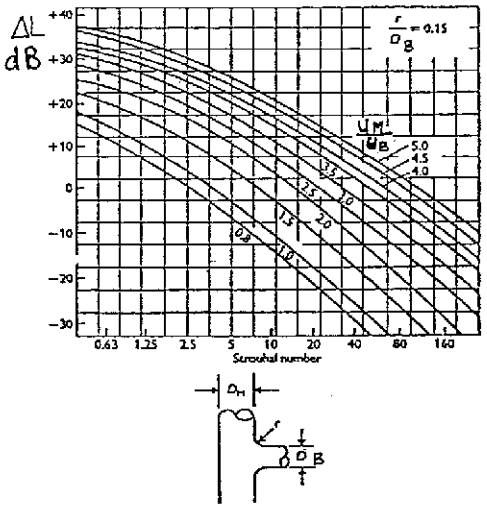

Figure 5f

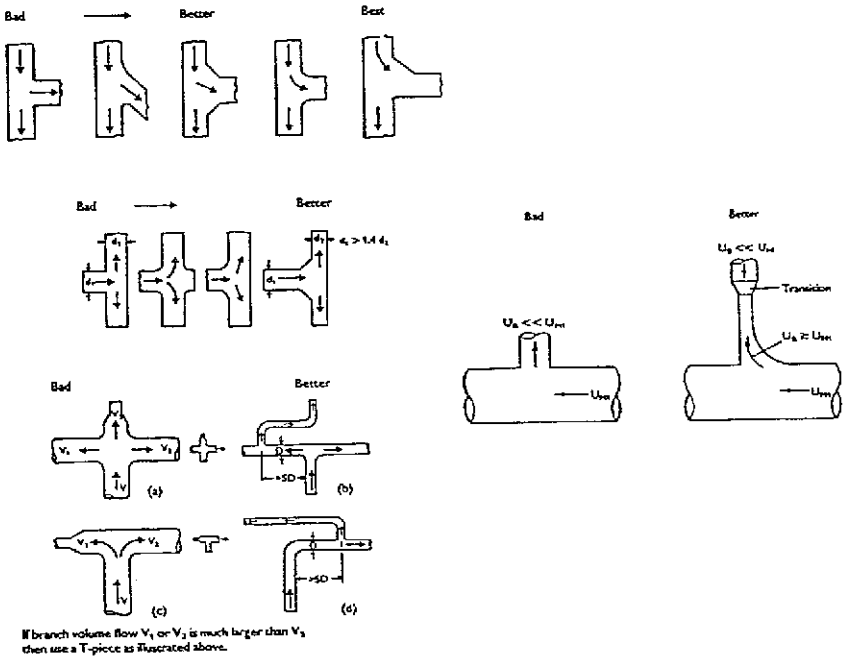

Figure 6

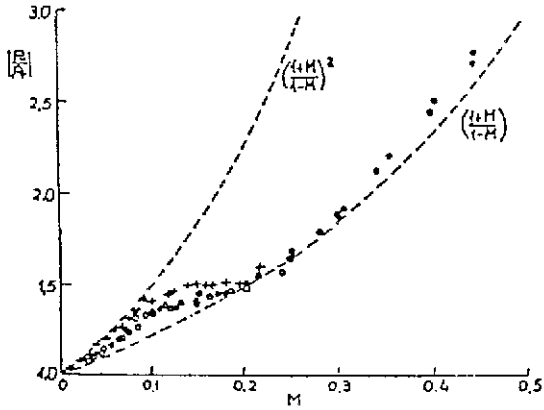

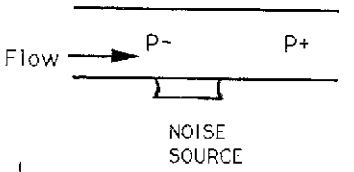

Mach number dependence of the measured ratio $\left|\frac{P-}{P+}\right|$ between the pressure amplitudes radiated in the upstream and downstream directions.

● 1477 Hz 0 = 1000 Hz + = 1000 Hz *(different location in the duct)*

Figure 7

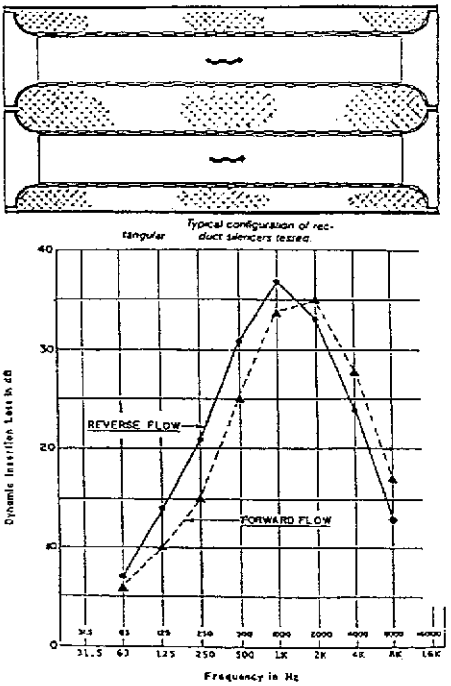

Figure 8

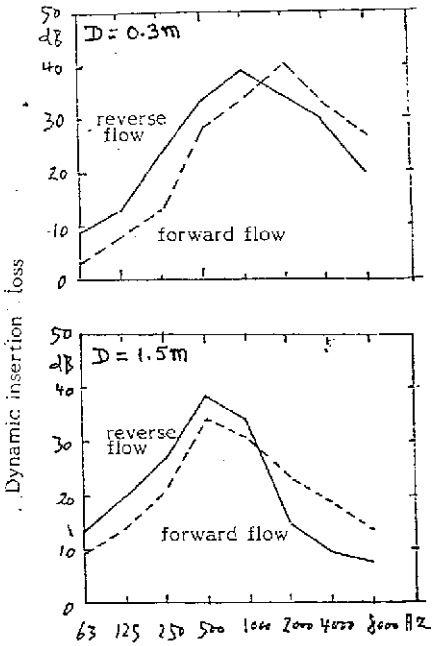

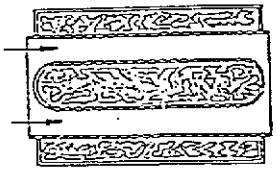

Typical cross-section of tubular conic flow silencers tested.

Figure 9

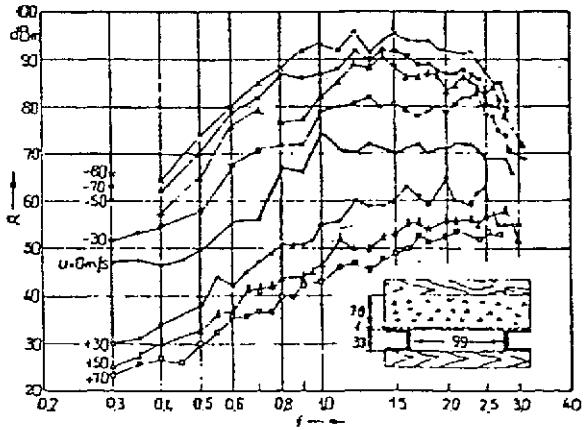

Attenuation α [dB/m] versus frequency f for mineral wool absorber with perforated facing plate
Parameter : flow velocity u (the passage way cut-of f frequency is about 4 kHz.)

Figure 10

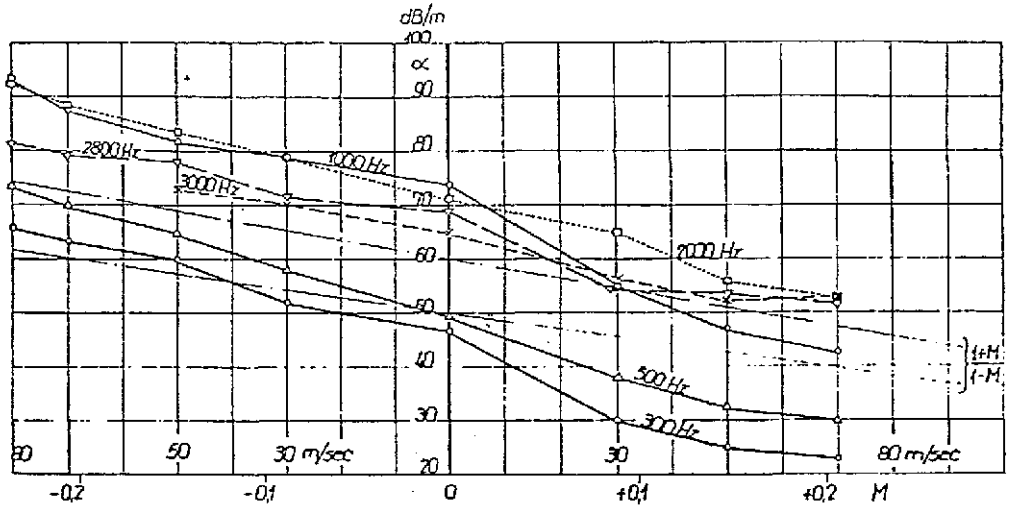

Attenuation α [dB/m] versus Mach number M with frequency as parameter.

Figure 11

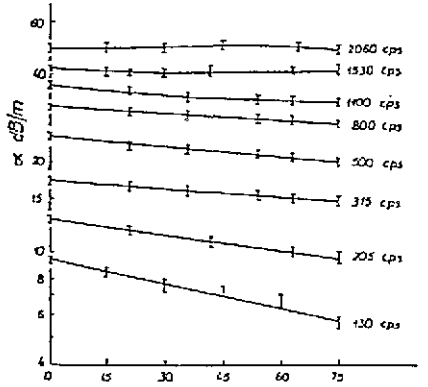

Midstream flow velocity, U_2 m/sec
forward flow

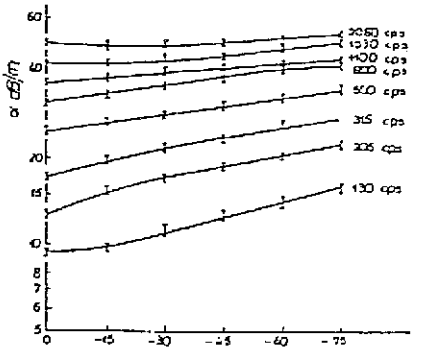

Midstream flow velocity U_2 m/sec
reverse flow

Experimental values of attenuation constant α as a function of midstream-flow velocity U, employing frequency as a parameter.

Figure 12

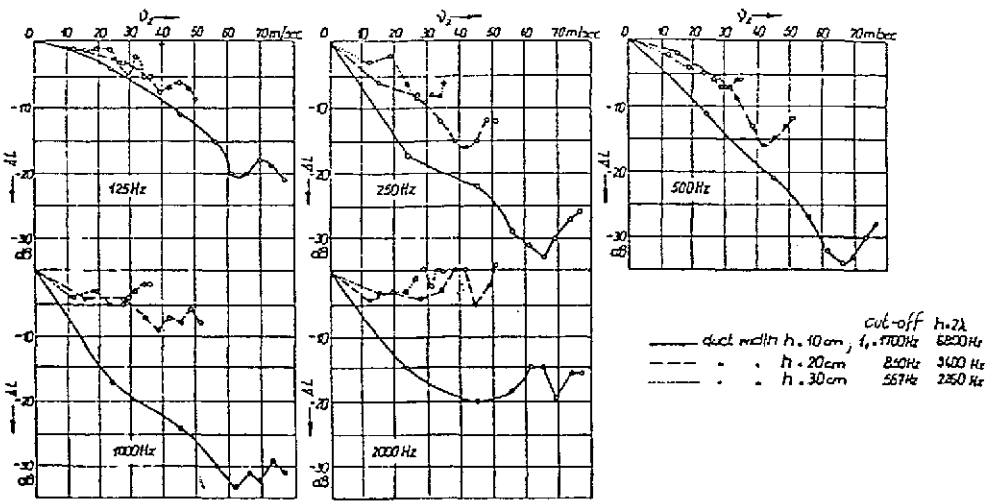

Attenuation loss in function of flow velocity for various frequencies.

Figure 13a

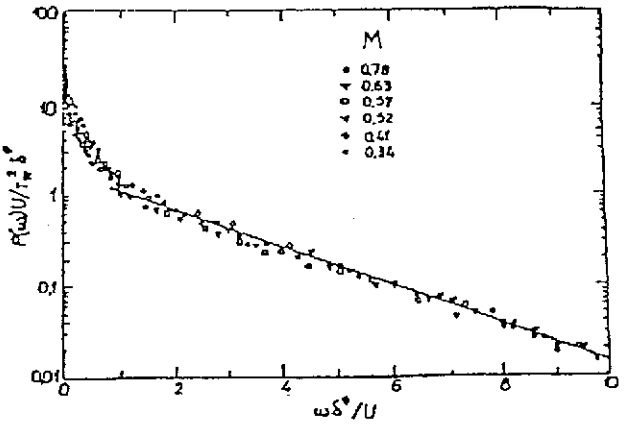

Dimensionless power spectrum of the wall pressure fluctuations

M , Mach number, $\zeta = \omega \delta^* / u$
δ^* , displacement thickness of boundary layer

Figure 13b

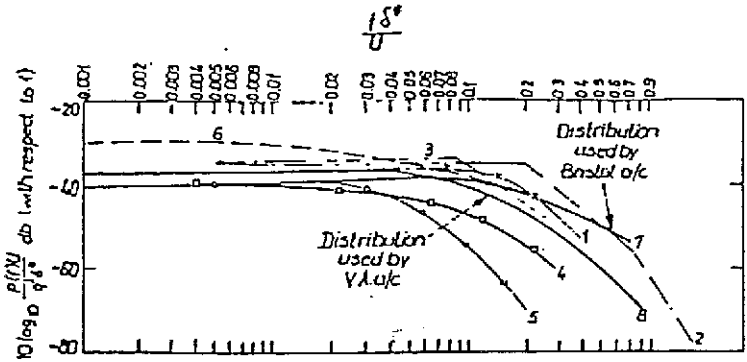

Frequency distribution of r m s pressure on boundary surface-scatter of data
P(f) = Spectral density of mean-square fluctuating pressure; u.free stream velocity,
σ boundary layer displacement thickness, f. frequency (cps),
q = 1/2 pu^2; p= free stream density wind tunnel : 1 Willmarth,
2 Harrison, 3 Bull; Flight: 4 Mc Lead and Jordon, 5 Muill and Algranli,
6 von Gierke; 7 Bull (10 January 1963); 8 Mean

Figure 14

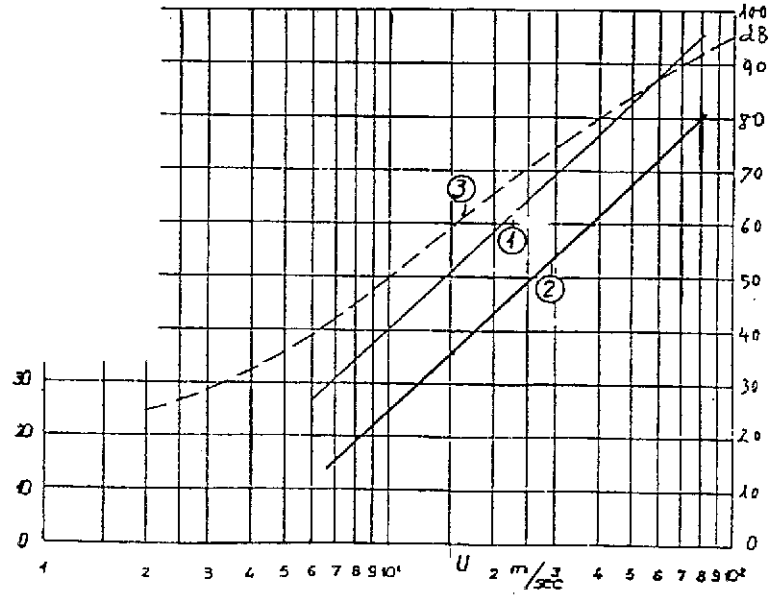

Calculated noise radiated by turbulent boundary layer
1. Without damping by the acoustic liner.
2. With damping by the acoustic liner.
3. Given by Gerber (1957).

Figure 15

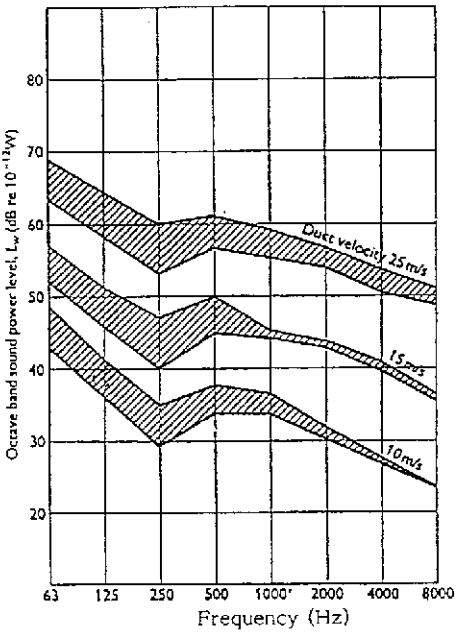

Sound power spectra of 600 mm x 600 mm straight empty steel duct for various air flow velocities.

As a general design guide, the following maximum duct velocities for conventional low velocity systems should not be exceeded.

NC design level	Main ducts	Branch ducts	Final run outs
20	4.5m/s	3.5m/s	2.0m/s
25	5.0m/s	4.5m/s	2.5m/s
30	6.5m/s	5.5m/s	3.25m/s
35	7.5m/s	6.0m/s	4.0m/s
40	9.0m/s	7.0m/s	5.0m/s

Figure 16

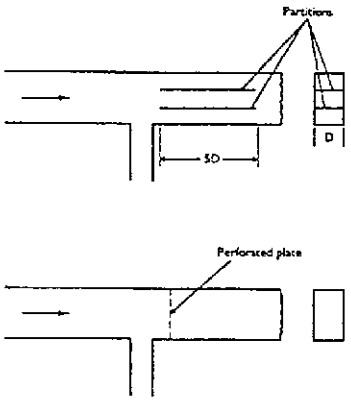

Measures to reduce the probability of drumming in large aspect ratio rectangular ducts.

Figure 17

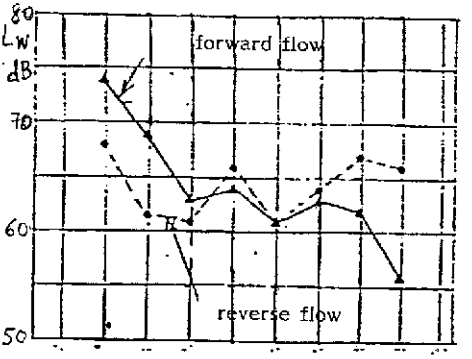

Frequency in Hz

Characteristic self-noise spectra for dissipative rectangular silencers at 40m/s passage. (For typical silencer configuration see Fig 7.)

Figure 18

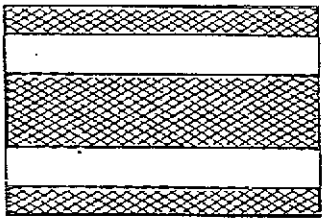

Flat-nosed rectangular silencer.

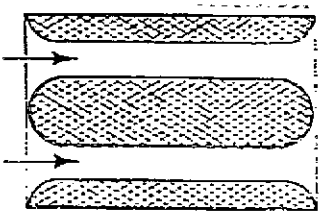

Round-nosed rectangular silencer.

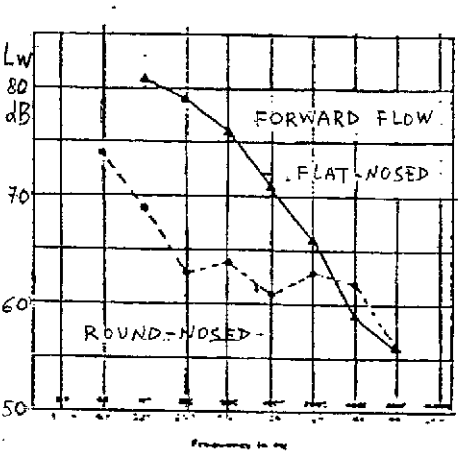

Self-noise spectra for "flat" and "round-nosed" rectangular splitter silencer at 40m/s passage forward flow mode.

Figure 19

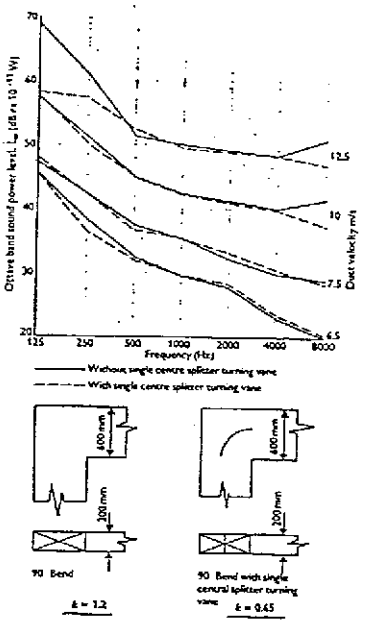

Sound power spectra produced by a 90° elbow in 600 mm x 200 mm duct with and without a single splitter turning vane.

Figure 20

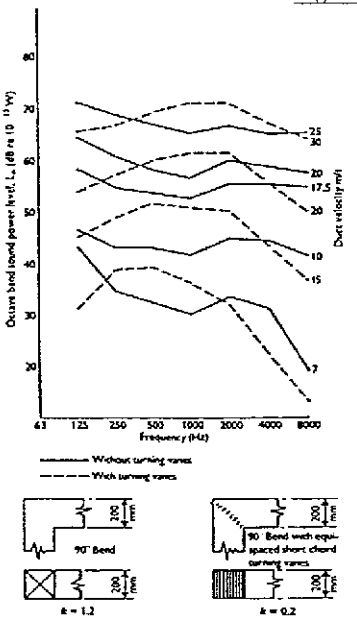

Sound power spectra produced by a 90° elbow in 600 mm x 200 mm duct system with and without short chord turning vanes.

Figure 21

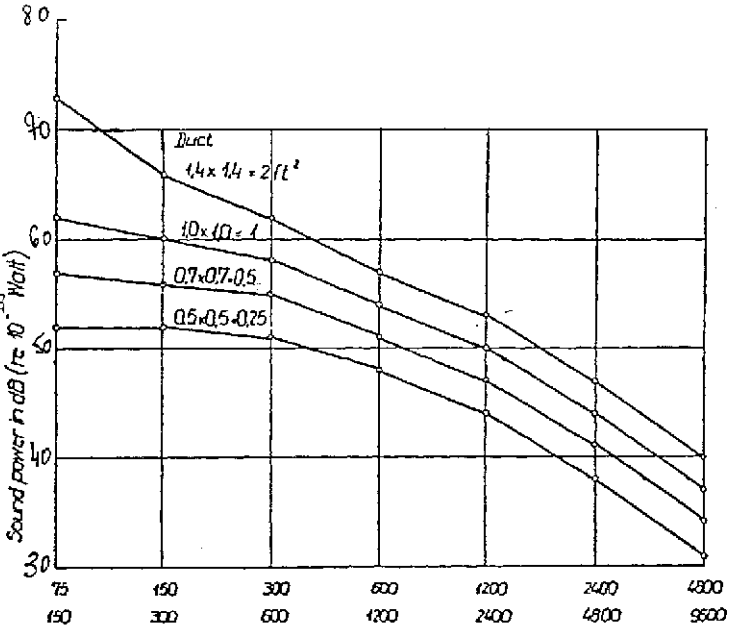

Approximale level of sound power generated by air flowing through elbows with turning vanes of 10 m/sec.

Figure 22 (continued) : Pressure loss coefficient of elbows

Elbow

Smooth radius with rectangular splitter vanes

One-splitter vane

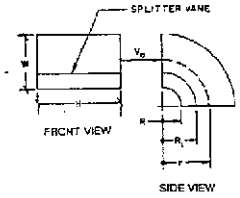

Two-splitter vanes

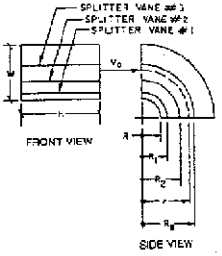

Coefficients for elbows with 1 splitter vane

			H/W										
R/W	*r/W*	*CR*	0.25	0.5	1.0	1.5	2.0	3.0	4.0	5.0	6.0	7.0	8.0
0.05	0.55	0.362	0.26	0.20	0.22	0.25	0.28	0.33	0.37	0.41	0.45	0.48	0.51
0.10	0.60	0.450	0.17	0.13	0.11	0.12	0.13	0.15	0.16	0.17	0.19	0.20	0.21
0.15	0.65	0.507	0.12	0.09	0.08	0.08	0.08	0.09	0.10	0.10	0.11	0.11	0.11
0.20	0.70	0.550	0.09	0.07	0.06	0.05	0.06	0.06	0.06	0.06	0.07	0.07	0.07
0.25	0.75	0.585	0.08	0.05	0.04	0.04	0.04	0.04	0.05	0.05	0.05	0.05	0.05
0.30	0.80	0.613	0.06	0.04	0.03	0.03	0.03	0.03	0.03	0.03	0.04	0.04	0.04

Coefficients for elbows with 2 splitter vanes

			H/W										
R/W	*r/W*	*CR*	0.25	0.5	1.0	1.5	2.0	3.0	4.0	5.0	6.0	7.0	8.0
0.05	0.55	0.362	0.26	0.20	0.22	0.25	0.28	0.33	0.37	0.41	0.45	0.48	0.51
0.10	0.60	0.450	0.17	0.13	0.11	0.12	0.13	0.15	0.15	0.17	0.19	0.20	0.21
0.15	0.65	0.507	0.12	0.09	0.08	0.08	0.08	0.09	0.10	0.10	0.11	0.11	0.11
0.20	0.70	0.550	0.09	0.07	0.06	0.05	0.06	0.06	0.06	0.06	0.07	0.07	0.07
0.25	0.75	0.585	0.08	0.05	0.04	0.04	0.04	0.04	0.05	0.05	0.05	0.05	0.05
0.30	0.80	0.613	0.06	0.04	0.03	0.03	0.03	0.03	0.03	0.03	0.04	0.04	0.04

Three - splitter vanes

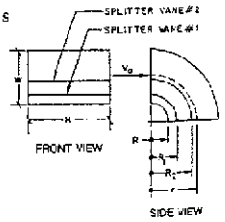

Coefficients for elbow with 3 splitter vanes

			H/W										
R/W	*r/W*	*CR*	0.25	0.5	1.0	1.5	2.0	3.0	4.0	5.0	6.0	7.0	8.0
0.05	0.55	0.467	0.11	0.10	0.12	0.13	0.14	0.16	0.18	0.19	0.21	0.22	0.23
0.10	0.60	0.549	0.07	0.05	0.06	0.06	0.06	0.07	0.07	0.08	0.08	0.08	0.09

Figure 22a: Pressure loss coefficient of elbows

Elbow

Smooth radius (die-stamped), round

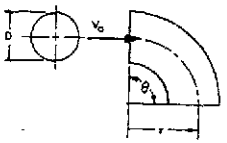

Coefficients for 90° Elbows						
r/D	0.5	0.75	1.0	1.5	2.0	2.5
ζ	0.71	0.33	0.22	0.15	0.13	0.12

Elbow

3, 4 and 5 pieces round

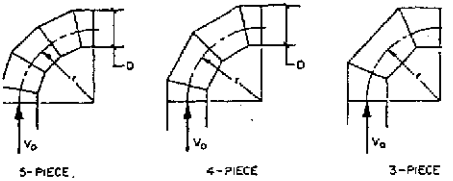

Coefficients for 90° Elbows				
No. of Pieces	r/D			
	0.75	1.0	1.5	2.0
5	0.46	0.33	0.24	0.19
4	0.50	0.37	0.27	0.24
3	0.54	0.42	0.34	0.33

Elbow

Mitered, round

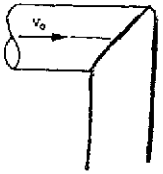

ζ = 1.2

Elbow

Mitered, rectangular

(Idelchik 1986, diagram 6-5)

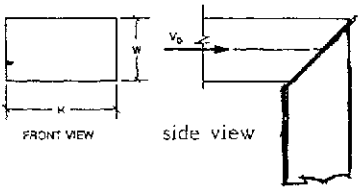

	H/W										
	0.25	0.5	0.75	1.0	1.5	2.0	3.0	4.0	5.0	6.0	8.0
ζ											

Elbow

Without vanes

Rectangular smooth radius

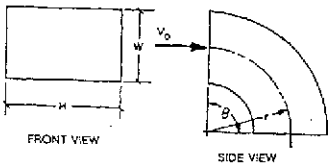

	H/W										
r/W	0.25	0.5	0.75	1.0	1.5	2.0	3.0	4.0	5.0	6.0	8.0
0.5	1.3	1.3	1.2	1.2	1.1	1.0	1.0	1.1	1.1	1.2	1.2
0.75	0.57	0.52	0.48	0.44	0.40	0.39	0.39	0.40	0.42	0.43	0.4
1.0	0.27	0.25	0.23	0.21	0.19	0.18	0.18	0.19	0.20	0.21	0.2
1.5	0.22	0.20	0.19	0.17	0.15	0.14	0.14	0.15	0.16	0.17	0.1
2.0	0.20	0.18	0.16	0.15	0.14	0.13	0.13	0.14	0.14	0.15	0.1

Figure 22b

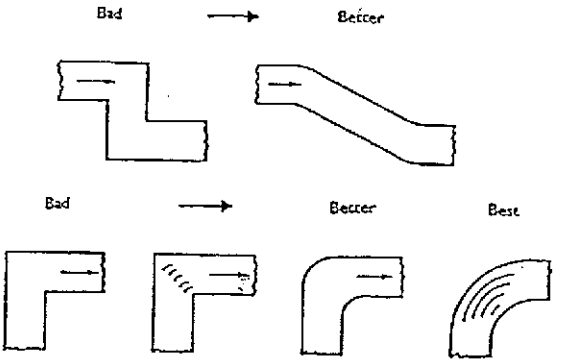

Note, however, that the mitred bend without turning vanes yields the highest reflection loss for the incident sound.

Guidelines for minimizing flow-generated noise in duct bends.

Figure 23

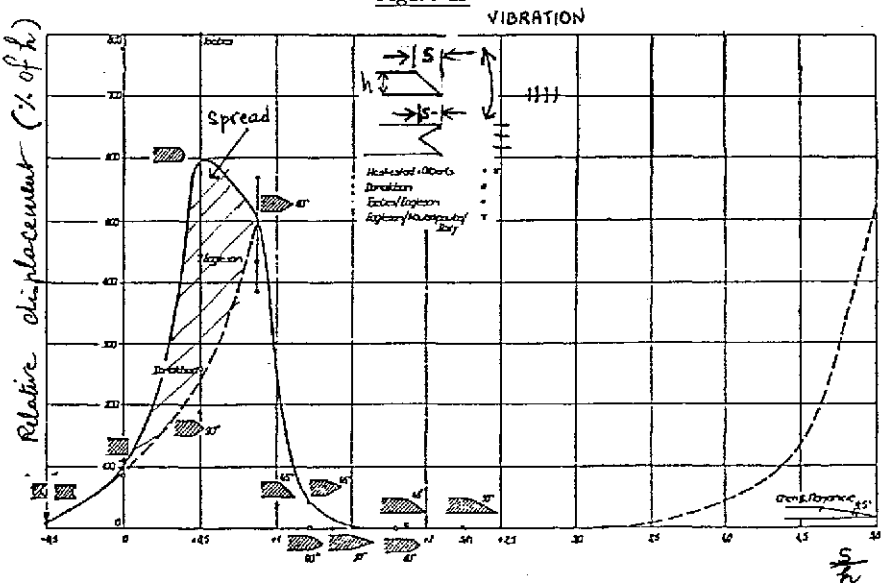

Karman-vortex induced vibration amplitude on plate as a function of its trailing edge parameter s/h (s distance from the flow separating part to the plate end; h plate thickness).

Figure 24

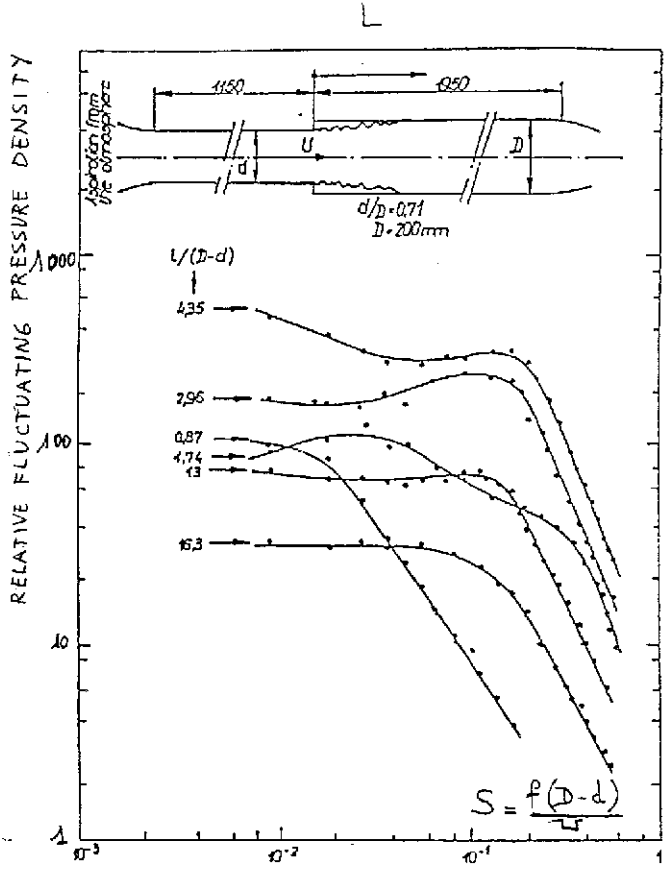

Spectra of the relative fluctuating pressure density of flow in a tube after sudden expansion.

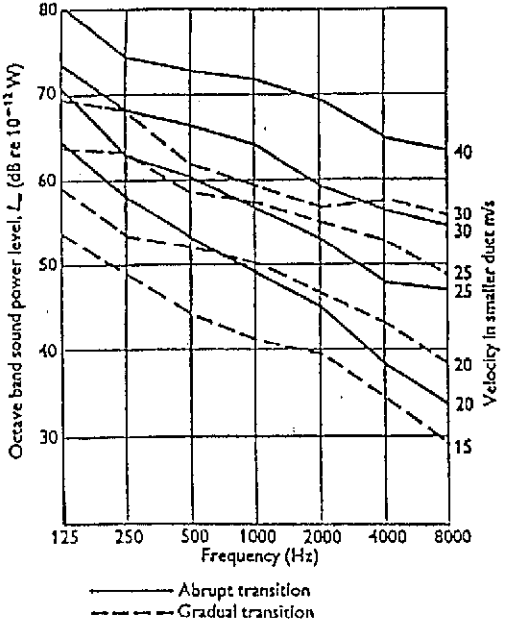

not bad arrangement

Sound-power levels of abrupt and gradual area transitions from 600 mm x 600 mm x 200 mm duct cross section (3.1).

No essential improvement

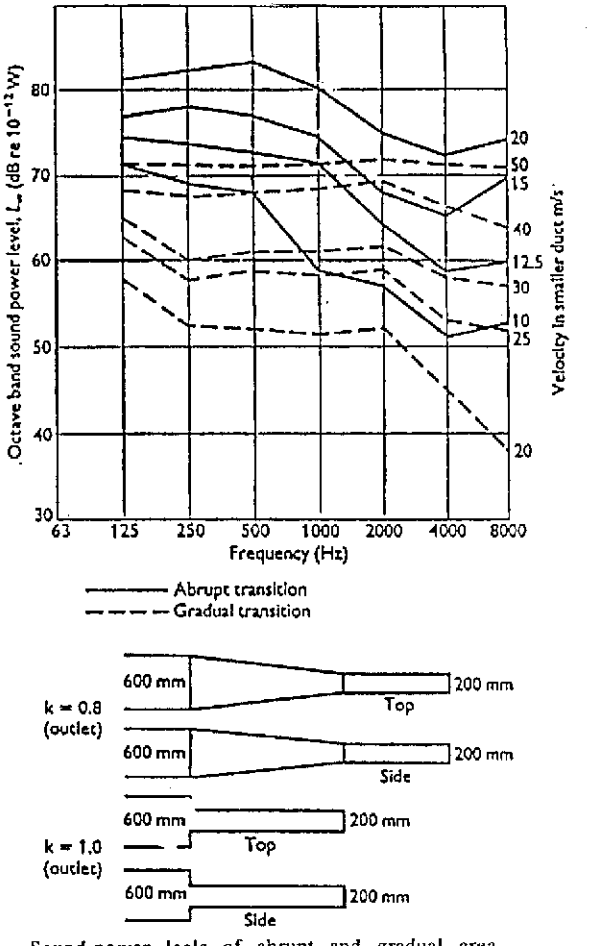

Sound-power levels of abrupt and gradual area transitions from 600 mm x 600 mm to 200 mm x 200 mm Duct cross sections (9:1)

Figure 25

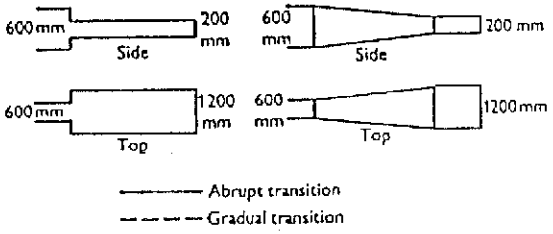

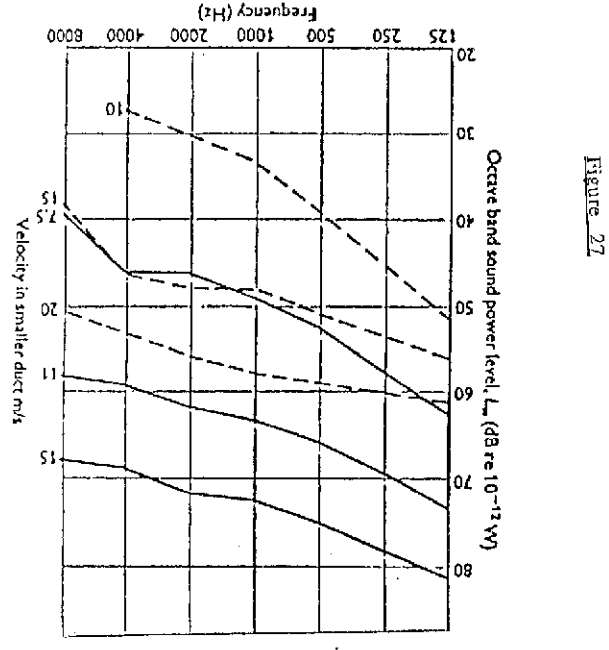

Figure 27

Poor performance due to expansion
Sound power levels of abrupt and gradual area transitions from 600 mm x 600 mm to 1200 x 200 mm duct cross section (1.5:1).
200 dB improvement

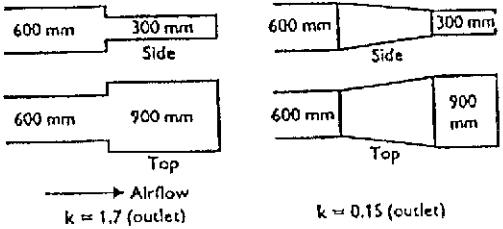

Abrupt transition
Gradual transition

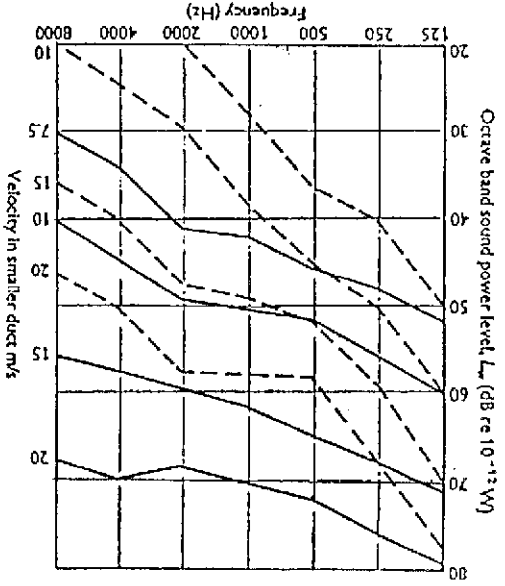

Figure 26

Poor performance due to expansion
Sound power levels of abrupt and gradual area transitions from 600 mm x 600 mm to 900 x 300 mm duct cross

Figure 28

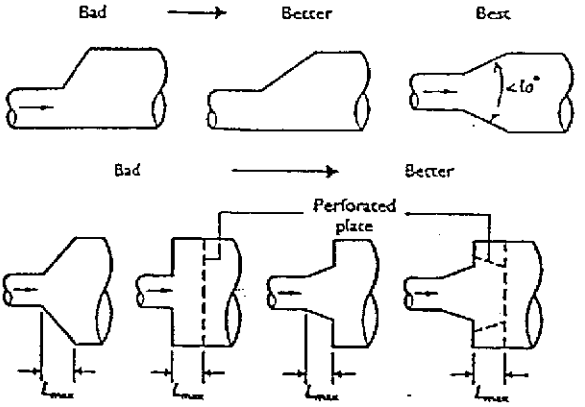

Guideliness for minimizing flow-generated noise at cross section changes

Figure 29

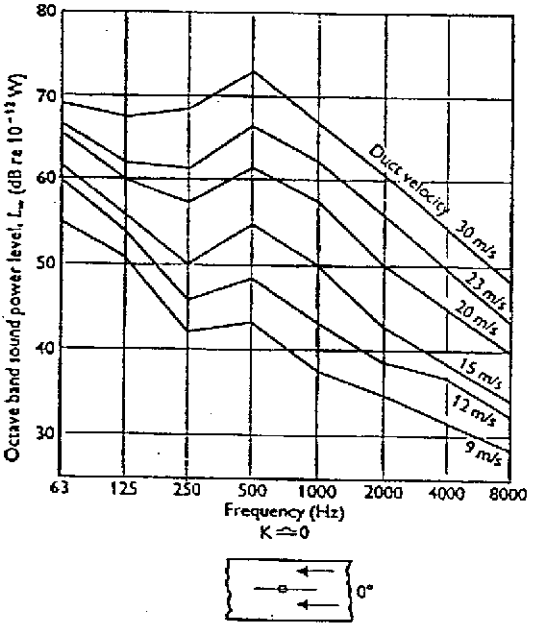

$$S = \frac{500 \cdot 0{,}02}{30} = 0{,}3$$

Karman vortex excitation at 30 m/s

500 Hz, λ = 600 mm

Sound power spectra producted by a single blade butterfly damper in a 600 x 600 mm duct at 0°, K is the aerodynamic loss factor.

Figure 30

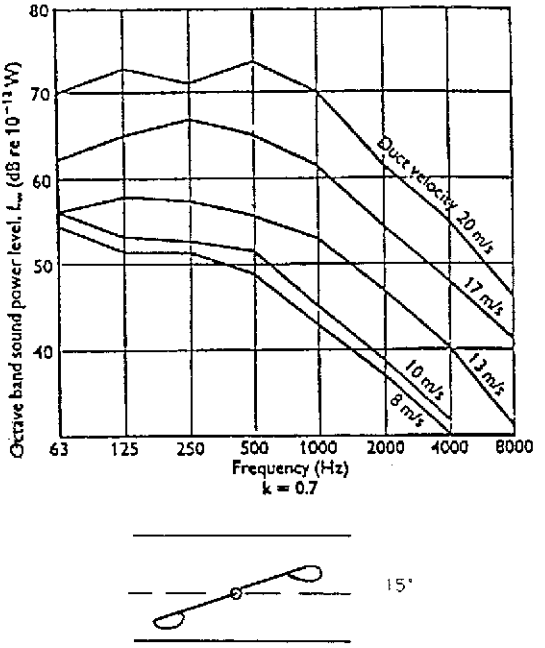

Nose bubble on the suction side

Sound power spectra produced by a single blade damper butterfly damper in a 600 x 600 mm duct at 15° : K is the aerodynamic loss factor.

Figure 31

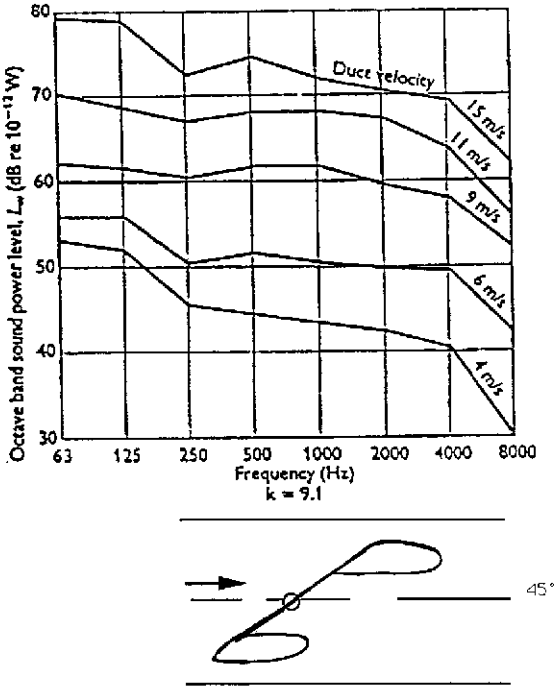

$$S_{gap} = \frac{500 \cdot 0.05}{100} = 0.25$$

Sound power spectra produced by a single blade damper butterfly damper in a 600 x 600 mm duct at 45° : K is the aerodynamic loss factor.

Figure 32

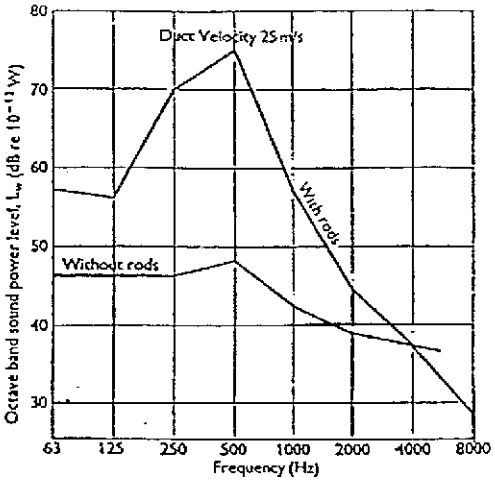

$$S = \frac{0{,}013 \cdot 500}{25} = 0.26$$

Sound power spectra of noise from a 600 x 600 mm duct with and without (4 13 mm Dia.) rods.

Figure 33

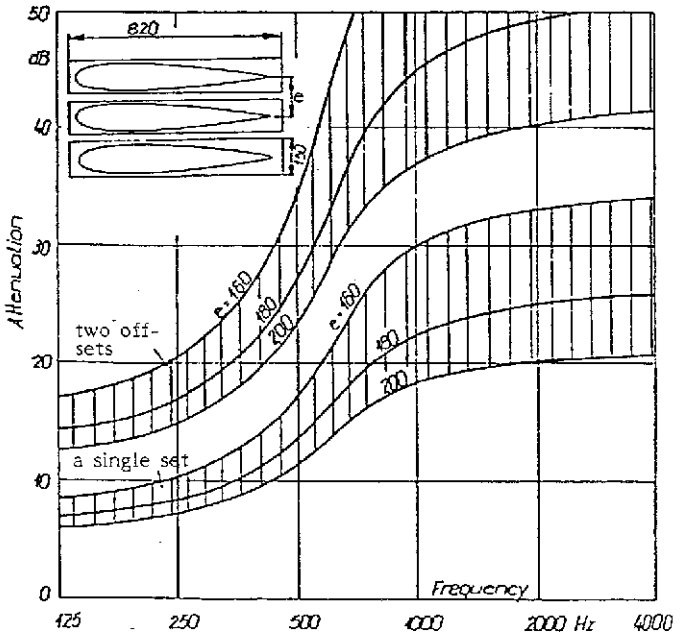

Stream-line-splitter silencer

Figure 34

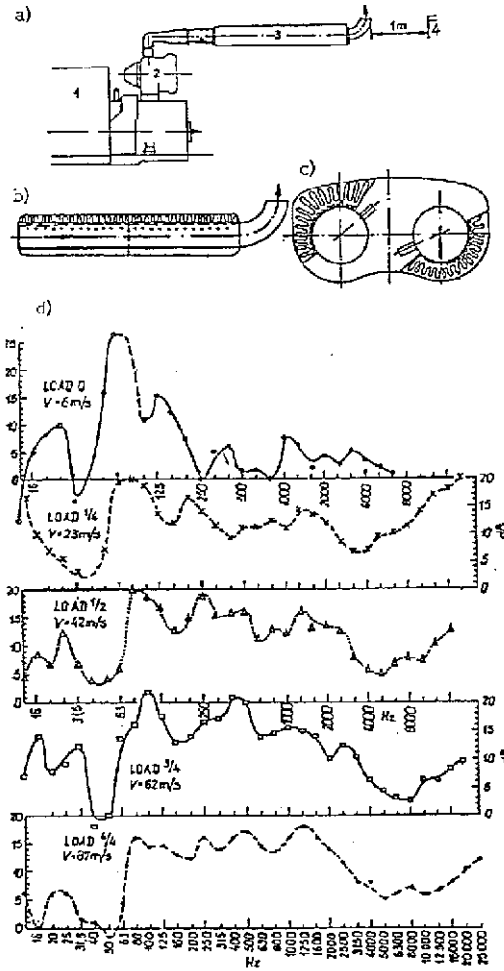

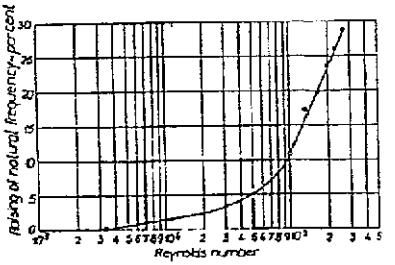

e)

Raising of the natural frequency of the resonator against the flow Reynolds number

a) Measuring rig.

1 - Four-stroke 12-cylinder diesel V-engine
2 - Turbocharger
3 - Silencer
4 - Microphone

b) Resonator-filter silencer consisting of two chambers in longitudinal section.

c) Resonator-filter silencer in cross-section.

d) Damping ability of the lined resonator-filter silencer in 1/3 octave band.

Figure 35

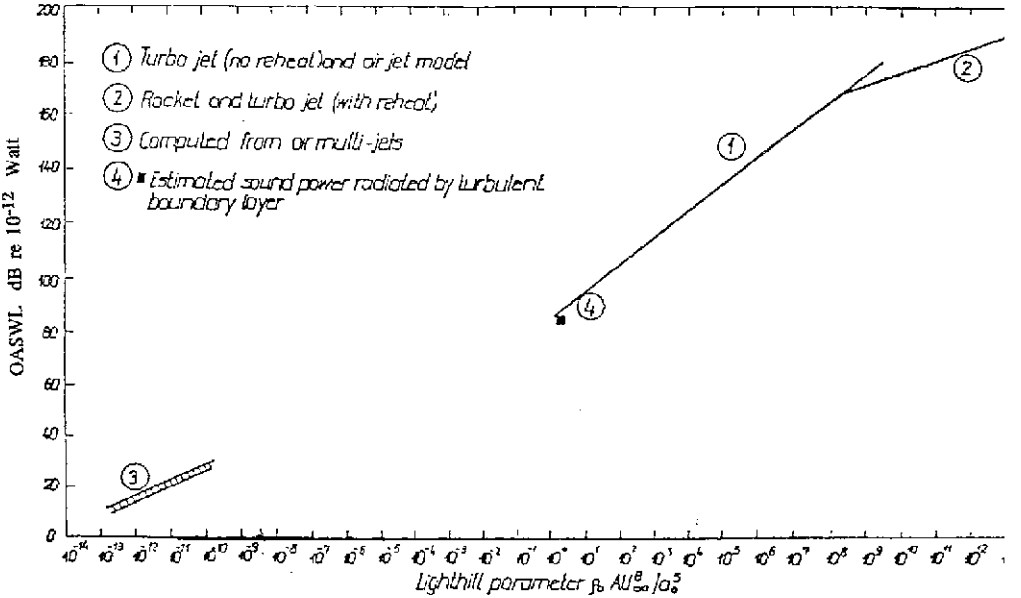

Overall sound power level of jet rocket and turbulent boundary layer as a function of the Lighthill parameter ρ_0 = density, a_0 = velocity of sound in the surrounding, A = area of duct

Figure 36

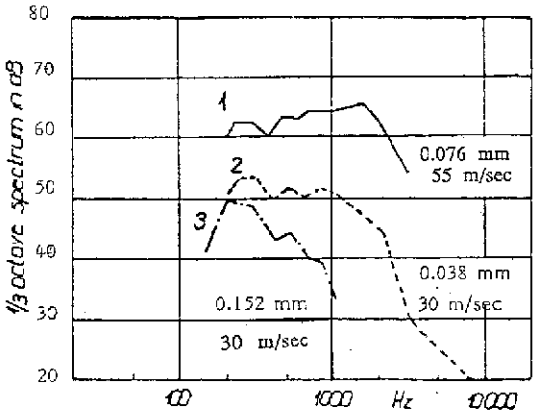

Spectrum of radiated total acoustic power (dB re 10^{-12}) 280 x 280 mm steel panel) due to vibration.

Clamped-clamped supported in a tunnel duct of (381 x 381 mm) Ratio between pond surface and duct section.

Plate thickness : 0.038 mm 0.076 and 0.152 mm